J Forensic Sci, July 2004, Vol. 49, No. 4
Paper ID JFS2003378
Available online at: www.astm.org

CASE REPORT

Emin Aghayev,[1] M.D.; Michael Thali,[1] M.D.; Christian Jackowski,[1] M.D.; Martin Sonnenschein,[2] M.D.; Kathrin Yen,[1] M.D.; Peter Vock,[2] M.D.; and Richard Dirnhofer,[1] M.D.

Virtopsy—Fatal Motor Vehicle Accident with Head Injury*

ABSTRACT: A man wearing no protective helmet was struck by a motor vehicle while riding a bicycle. He was loaded on his left side, and the impact point of his head was his occiput on the car roof girder. He was immediately transported to the general hospital, where he passed away. Postmortem examination using multi-slice computed tomography (MSCT) revealed an extensively comminuted fracture of the posterior part and the base of the skull. Observed were deep direct and contrecoup brain bruises, with the independent fractures of the roof of the both orbits. Massive subdural and subarachnoidal hemorrhage with cerebral edema and shifting of the mid-line towards left side were also detected. MSCT and autopsy results were compared and the body injuries were correlated to vehicle damages. In conclusion, postmortem imaging is a good forensic visualization tool with great potential for documentation and examination of body injuries and pathology.

KEYWORDS: forensic science, forensic radiology, digital autopsy, virtual autopsy, virtopsy, computed tomography (CT), postmortem, fracture of the base of the skull, ring fracture

Skull fractures are reported to occur in 50% (1) of fatal road accidents and in 70 to 72% (1,2) of fatal cases of blunt head trauma due to multiple causes. Most (80 to 92%) (3,4) of the skull fractures seen in this context involve the base of the skull. The condition and direction of most skull fractures correlate well with the site of impact (3,5–7) and are thus of medicolegal significance in cases where the impact site is to some extent in question.

The classical X-ray examinations often fail to show fractures of the base of the skull, especially where routine projections are utilized (8). Multi-slice computer tomography (MSCT) and magnetic resonance imaging (MRI), which have seen major developments in the last years (9,10), provide a significant help in the diagnosis of bone and soft tissue injuries in vivo.

The enormous possibilities of true sections, of 2D/3D image reconstruction and of presentation using MSCT and MRI data are clearly superior to conventional, purely descriptive methods. The first systematic experience in postmortem visualization by MSCT, MRI and their combination was already reported by the Institutes of Forensic Medicine and Radiology of the University of Bern (11–14). Until the month of October 2003, we have used MSCT and MRI as auxiliary radiological examination methods for postmortem evaluation and diagnosis in 85 cases.

Here we report the first case of fatal blunt head trauma with reconstructive correlation of body injuries to vehicle damages documented by postmortem CT and autopsy.

[1] Institute of Forensic Medicine, University of Bern, Buehlstrasse 20, 3012 Bern, Switzerland.
[2] Institute of Diagnostic Radiology, Inselspital Bern, 3010 Bern, Switzerland.
* Supported by grant from Gerbert Ruef Foundation, Switzerland.
Received 8 Nov. 2003; and in revised form 13 and 15 Mar. 2004; accepted 15 Mar. 2004; published 26 May 2004.

Material and Methods

Case

A 72-year-old white male without a protective helmet was struck by a motor vehicle from his left and posterior side. He was loaded on his left side and the impact point of his head was posteriorly. His occiput was struck on the car roof girder and the skull was compressed in posterior-anterior direction. The car roof girder was displaced backwards by 20 cm (Fig. 1*c*). After the accident, he was immediately transported to a local hospital. The skull was trepanated, and a ventricular probe was inserted. The man died 21 h after the accident, due to high intracranial pressure and brain edema. Multi-slice computed tomography (MSCT) was performed 6 h postmortem, and an autopsy was carried out 24 h after death.

Radiological and Autopsy Examinations

For radiological examination, the body was wrapped in two radiologically artefact-free body bags (Rudolf Egli G, Bern, Switzerland). MSCT scanning was carried out on a GE Lightspeed QX/I unit (General Electric, Milwaukee, WI). Axial MSCT was performed using a collimation of 4 × 1.25 mm; 950 axial cross sections were calculated from the volume data. The duration of MSCT scanning was 10 min. On a workstation (Advantage Windows 4.1, General Electric Medical Systems, Milwaukee, WI), sagittal and coronal reformations and three-dimensional reconstruction in Shaded Surface Display (SSD), Volume Rendering (VR) (Fig. 2*a, b*) and Transparent Bones (TB) (Fig. 5) protocols were obtained.

The autopsy was performed by board-certified forensic pathologists. MSCT and autopsy results were compared. The body injuries were correlated to vehicle damage.

Copyright © 2004 by ASTM International, 100 Barr Harbor Drive, PO Box C700, West Conshohocken, PA 19428-2959.

FIG. 1—*Car damages: a) impact point of the left hip region (thick arrow); b) impact point of the left trunk (dotted arrow); c) car roof girder was dislocated 20 cm backwards (double arrow); and d) scrub marks on the right front door of the car caused by bicycle (two thin arrows).*

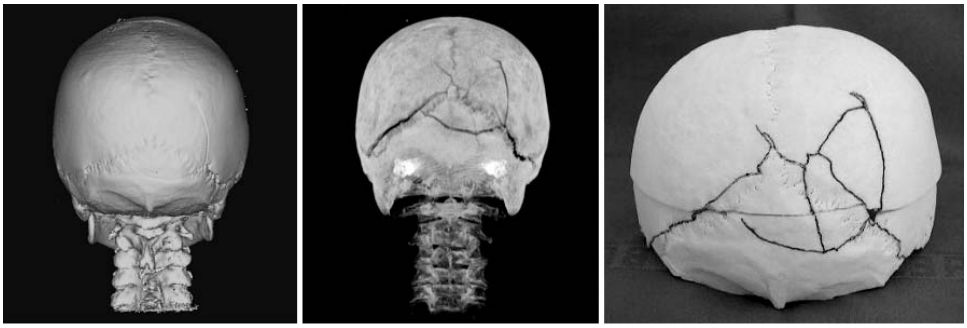

(a) (b) (c)

FIG. 2—*a) 3D bone reconstruction using the Shaded Surface Display protocol. The gaps of the fractures are insufficiently demonstrated; b) 3D bone reconstruction using the Volume Rendering protocol with adapted parameters. The more correct presentation of the gaps of the fracture system is obvious; and c) photograph of the macerated parieto-occipital skull with extensive fractures.*

Results

Radiological Findings by MSCT Examination

Head Injury—Computer tomography of the soft tissues of the head showed subcutaneous occipital hematoma (Fig. 3), with massive subdural and subarachnoidal hemorrhage over both cerebral hemispheres (Fig. 4*a*) and minor hemorrhage over the cerebellum. Deep occipital and fronto-basal brain bruises were diagnosed (Fig. 4*a*). Furthermore two circular, approximately 5 mm large hemorrhages of caudate nuclei were detected, symmetrically located adjacent to the ventricular probe (Fig. 4*a*). Shifting of the mid-line structures towards the left side, as a sign of elevated intracranial pressure and cerebral swelling, was also present. MSCT, by its geometric resolution, was able to depict clearly the bent fracture of the occiput and the ring fracture of the base of the skull, which both corresponded to one impact point in the occiput (Figs. 2, 5). Independent fractures of the roof of both orbits were diagnosed (Fig. 3). From the MSCT dataset, the head was visualized in 2D and 3D. On the workstation, soft tissues were electronically eliminated, based on the difference in tissue densities. The result was a 3D SSD and VR presentation of the bony skull (Fig. 2*a, b*).

Other Lesions—Radiological examination of the thoracic, abdominal, pelvic regions and extremities were also undertaken.

The virtual autopsy examination of the soft tissues of the back revealed large hemorrhages in the subcutaneous fat tissue and in the muscles of the left and right shoulder, left and right lateral hip region and on the left lateral trunk side (Fig. 6*c*). Minor hemorrhages of the subcutaneous fat tissue of right shoulder and right hip region were also detected.

Forensic Findings at Autopsy

Autopsy confirmed the above-mentioned radiological findings. The ring fracture of the base of the skull as well as the bent fracture of the occiput with the subcutaneous hemorrhage were diagnosed. The massive subdural and subarachnoidal hemorrhage over both cerebral hemispheres and minor hemorrhage over the cerebellum were seen. The nearly symmetrical located hemorrhages of both caudate nuclei were also detected (Fig. 4*b*). Furthermore, independent fractures of the roof of both orbits as well as brain bruises in occipital and frontal lobes were diagnosed. Generalized swelling of whole brain, within the severe craniocerebral injury, with the shifting of the mid-line towards the left side was present. In addition to the MSCT findings, brain stem hemorrhage between the pons and the medulla oblongata was discovered.

Soft tissue section revealed large hemorrhages of the subcutaneous fat tissue and muscles of the left and right shoulder, left and

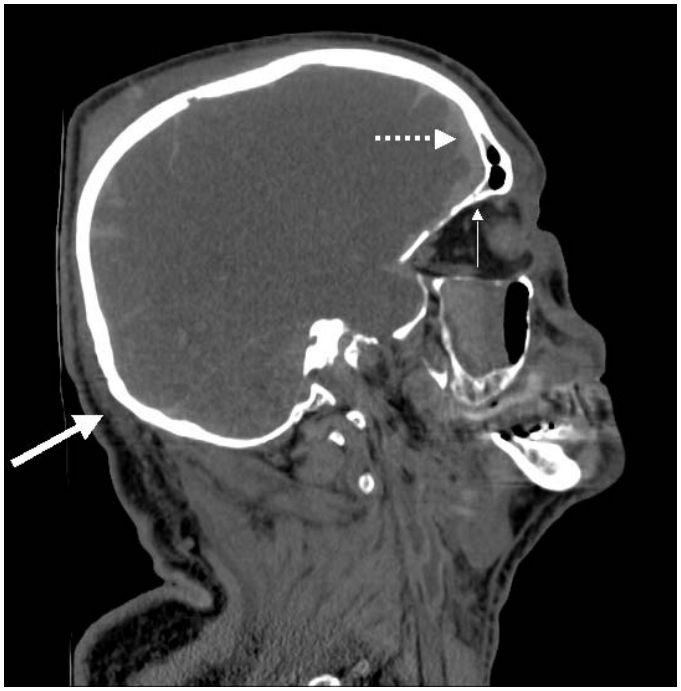

FIG. 3—*Right paramedian sagittal 2D reformation shows the extracerebral subdural and subarachnoidal hematoma (dotted arrow), the fracture of the roof of the orbit (thin arrow) and the occipito-basal subcutaneous hemorrhage (thick arrow).*

right lateral hip region and on the left lateral trunk side (Fig. 6*a, b*) as well as minor hemorrhages on the right shoulder and right hip region.

The histological examination for fat embolism of the lung was positive.

Discussion

Head Injuries

Although the mechanism of formation of ring fractures of the base of the skull is well known from the publications of Messerer, Patscheider, Gurdjian and Vondra, it was difficult to analyze and classify this combined fracture (6,7,15,16). We divided the mechanism of formation of this fracture into two components occurring in parallel.

The first component was the direct impact of the car roof girder on the occiput, which caused a mosaic or spider's web fracture of the occiput (17). Subcutaneous occipital hematoma accompanied it. Also, the car roof girder was displaced backwards by 20 cm (Fig. 1*c*). This impact point caused the direct and contrecoup brain injuries (7). The various hemorrhages in the frontal lobe, frontobasal brain bruises and the fractures of the roof of both orbits were judged to be the contrecoup brain injuries. The deep occipito-basal brain bruises and the brain tissue pinched in the gap of the temporal fracture were thought to represent the direct injury. Two symmetrical hemorrhages of the caudate nuclei, located directly by ventricular probe were the result of the direct trauma by the manipulation with the pressure probe during the urgent treatment.

The second component was the compression along the vertebral column through the loading of the body on the car hood. At this moment, the head was accelerated backwards and downwards, and the base of the skull fractured in ring form (16). The second component is most typical in the formation of ring fractures caused by compression of the skull and vertebral column in the cranio-caudal direction (6,7,16,18,19). Both of these components were ongoing as one combined movement. In this case, the hemorrhage of the brain stem, between pons and medulla oblongata was secondary to the head injury, and occurred after increased intracranial pressure and the following skull trepanation (20,21).

Correlation of Body Injuries to the Car Damages

There were no macroscopic biological tissue traces on the car. MSCT of the soft tissues of the back showed intensive hemorrhage of the fat tissue and muscles over the left shoulder, trunk and hip region. There were also minor hemorrhages on the right shoulder and right hip region. All these findings were diagnosed on the soft tissue sections of the back and they evidenced that the body was loaded at first with the left side on the hood of the car. It was the impact of major energy. The damage to the bicycle, especially the saddle and the handlebar, which were turned to the left side, also verify the point of impact being the left side of the bicycle. There were also two scrub marks on the right front door of the car, at the level of the doorknob, which were caused by the bicycle (Fig. 1*d*).

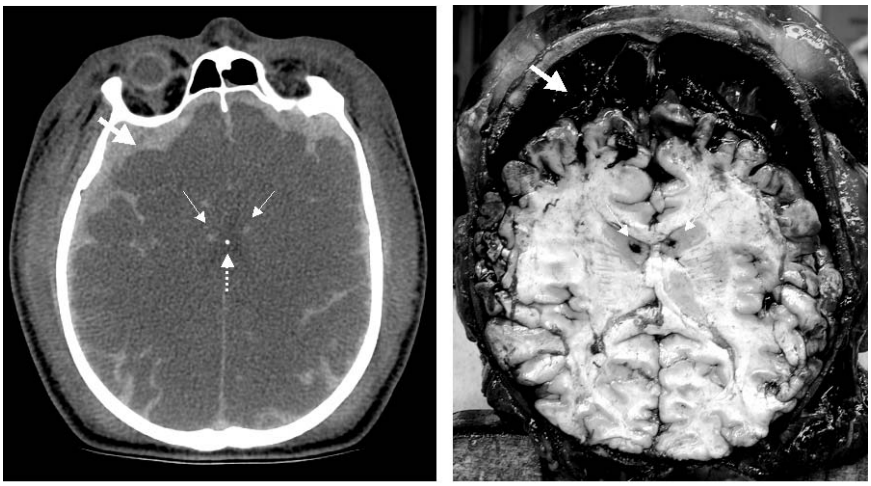

(a) (b)

FIG. 4—*Massive subdural hematoma (thick arrow), symmetrically located hemorrhages within the caudate nuclei (thin arrows) and tiny pressure probe inside the ventricle (dotted arrow). Correlation of brain injuries: a) in CT and b) in autopsy.*

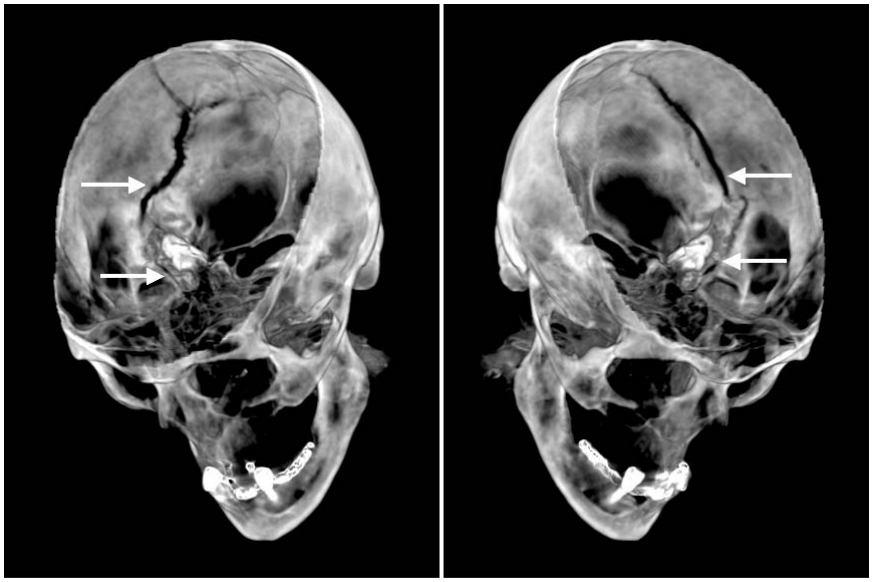

(a) (b)

FIG. 5—*Ring fracture (arrows): a) cranio-caudal left oblique perspective and b) cranio-caudal right oblique perspective.*

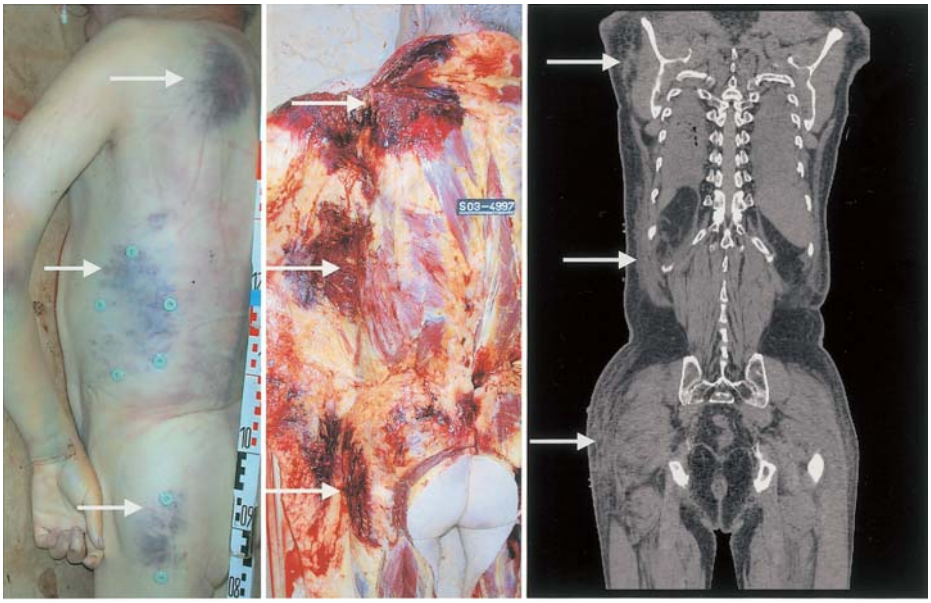

FIG. 6a FIG. 6b FIG. 6c

FIG. 6—*Correlation of subcutaneous fat tissue injury, muscle bruise and hemorrhage of the left shoulder, left trunk and left hip regions (arrows). The injured regions were pointed out with radiologically visible skin markers: a) photograph with markers before forensic analysis; b) left posterior oblique view during autopsy; and c) coronal reformation from MSCT data.*

After the loading on the hood, the man struck his head on the roof girder of the car, as evidenced by the backward dislocation of 20 cm of the car roof girder (Fig. 1*c*). After the loading on the roof, the man fell to the ground on the right, back side of the car.

In summary, the hemorrhages of the soft tissues of shoulder, trunk and hip regions of the left side and the fracture of the occiput with subcutaneous fat tissue hemorrhage were the impact injuries, and the minor hemorrhages of the soft tissues of the right shoulder and right hip regions were the secondary injuries caused by falling of the body to the ground.

Virtual Autopsy Using MSCT

Only the recent radiological development of cross-sectional imaging has allowed volumetric data sampling, and this became a basis to implement the modern radiological examination methods in forensic medicine. It is known from clinical experience, that classical radiography alone often fails to demonstrate fractures of the base of the skull, especially where routine projections are utilized (8). The introduction of the spiral CT technique by Vock and Kalender (1990) and the currently four-fold expansion of detector arrays (MSCT since 1998) allow for rapid accurate localization,

isotropic documentation and for demonstration of the pattern of injury (9,10,22–24). This is an absolute and important advantage of MSCT over classical X-rays examination. The possibility of non-destructive postmortem 2D and 3D reconstruction of bone, soft tissue and whole organ injuries and pathologies enhances the potential of volume scanning (11–14,25,26). 3D reconstructions using the VR (Fig. 2*b*) and TB (Fig. 5) protocols showed the skull fractures more precisely than the SSD protocol (Fig. 2*a*). The explanation for the difference in these 3D protocols is that the diverse algorithms of the SSD protocol responsible for polishing and smoothing the 3D surface, result in a loss of resolution of bone fissures and nondislocated fractures (Fig. 4*a*). SSD just presents the surfaces of different tissues based on a density threshold whereas VR keeps the entire set of 3D data.

Except for the petechial hemorrhages in the basal part of the frontal lobe and the hemorrhage in the brain stem, in our case all tissue injuries revealed by autopsy were also demonstrated by MSCT. As it is well known from clinical experience, magnetic resonance imaging (MRI) has a more detailed and exact soft tissue resolution and is especially useful for the assessment of brain injuries (21,27). Unfortunately, this examination was not performed in our case for logistic reasons. Firsching (2002) already reported that computed tomography (CT) failed to show brain stem lesions, and neuropathological data were only available from autopsies. In his study with 100 patients, brain stem affection was seen in 52% of MRI examinations (21). Our experience with postmortem imaging with CT and MRI also shows the superiority of MR imaging in brain injuries.

In conclusion, postmortem imaging is an excellent forensic visualization tool with a great potential for the detection and documentation of injuries. MSCT is the preferred method for bone pathology and is good to fair for soft tissue pathology where MRI, despite it's more complicated and expensive technology and longer acquisition times, is often superior.

Acknowledgments

We are grateful to Elke Spielvogel (Department of Radiology, University Hospital of Bern), and also to Roland Dorn and Urs Koenigsdorfer (Institute of Forensic Medicine, University of Bern) for their excellent help in data acquisition during the radiologic examination and the forensic autopsy. Particular thanks go to Erich Graser for his distinguished support in analyzing and reconstructing the accident.

References

1. Sevitt S. Fatal road accidents. Injuries, complications, and causes of death in 250 subjects. Br J Surg 1968;55(7):481–505. [PubMed]
2. Freytag E. Autopsy findings in head injury from blunt forces. Arch Pathol 1963;75:402–13. [PubMed]
3. Vance BM. Fractures of the skull—complications and causes of death: a review of 512 necropsies and of 61 cases studied clinically. Arch Surg 1927;14:1023–92.
4. LeCount ER, Apfelbach CW. Pathologic anatomy of traumatic fractures of cranial bones—and concomitant brain injuries. JAMA 1920;74:501–11.
5. Hooper R. Injuries of the skull. In: Patterns of acute head injury. Baltimore: Williams and Wilkens, 1969:21–30.
6. Vondra J. Fractures of the base of the skull. Springfield: Charles C. Thomas, 1965.
7. Gurdjian ES. Impact head injury. Springfield: Charles C. Thomas, 1975.
8. Russel WR, Schiller F. Crushing injuries to the skull: clinical and experimental observations. J Neurol Neurosurg Psychiatry 1949;12:52–60.
9. Fuchs T, Kachelriess M, Kalender WA. Technical advances in multi-slice spiral CT. Eur J Radiol 2000;36(2):69–73. [PubMed]
10. Kalender WA. Computed tomography. New York: Wiley, 2000.
11. Thali MJ, Yen K, Schweitzer W, Vock P, Boesch C, Ozdoba C, et al. Virtopsy, a new imaging horizon in forensic pathology: virtual autopsy by postmortem multislice computed tomography (MSCT) and magnetic resonance imaging (MRI)—a feasibility study. J Forensic Sci 2003;48(2):386–403. [PubMed]
12. Thali MJ, Yen K, Plattner T, Schweitzer W, Vock P, Ozdoba C, Dirnhofer R. Charred body: virtual autopsy with multi-slice computed tomography and magnetic resonance imaging. J Forensic Sci 2002;47(6):1326–31. [PubMed]
13. Thali MJ, Schweitzer W, Yen K, Vock P, Ozdoba C, Spielvogel E, et al. New horizons in forensic radiology: the 60-second digital autopsy-full-body examination of a gunshot victim by multislice computed tomography. Am J Forensic Med Pathol 2003;24(1):22–7. [PubMed]
14. Thali MJ, Schwab CM, Tairi K, Dirnhofer R, Vock P. Forensic radiology with cross-section modalities: spiral CT evaluation of a knife wound to the aorta. J Forensic Sci 2002;47(5):1041–5. [PubMed]
15. Messerer O. Experimentelle Untersuchungen ueber Schaedelbrueche. Muenchen: M. Rieger, 1884.
16. Patscheider H. Zur Entstehung von Ringbrüchen des Schaedelgrundes. Dtsch Z ges gerichtl Med 1961;52:13–21.
17. Knight B. Forensic pathology. London: Edward Arnold, 1991.
18. Spasic P, Rezic A. (The mechanism of ring-fractures of the base of the skull). Z Rechtsmed 1970;67(5):324–8. [PubMed]
19. Voigt GE, Skold G. Ring fractures of the base of the skull. J Trauma 1974;14(6):494–505. [PubMed]
20. Parizel PM, Makkat S, Jorens PG, Ozsarlak O, Cras P, Van Goethem JW, et al. Brainstem hemorrhage in descending transtentorial herniation (Duret hemorrhage). Intensive Care Med 2002;28(1):85–8. [PubMed]
21. Firsching R, Woischneck D, Klein S, Ludwig K, Dohring W. Brain stem lesions after head injury. Neurol Res 2002;24(2):145–6. [PubMed]
22. Kalender WA, Vock P, Polacin A, Soucek M. [Spiral-CT: a new technique for volumetric scans. I. Basic principles and methodology]. Rontgenpraxis 1990;43(9):323–30. [PubMed]
23. Soucek M, Vock P, Daepp M, Kalender WA. [Spiral-CT: a new technique for volumetric scans. II. Potential clinical applications]. Rontgenpraxis 1990;43(10):365–75. [PubMed]
24. Balfe DM, Ehman RL. The society of computed body tomography and magnetic resonance imaging. Research in CT and MR imaging: 2000 and beyond. Radiology 1998;207(3):561–4. [PubMed]
25. Brogdon BG. Forensic radiology. Boca Raton: CRC Press, 1998.
26. Calhoun PS, Kuszyk BS, Heath DG, Carley JC, Fishman EK. Three-dimensional volume rendering of spiral CT data: theory and method. Radiographics 1999;19(3):745–64. [PubMed]
27. Snow RB, Zimmerman RD, Gandy SE, Deck MD. Comparison of magnetic resonance imaging and computed tomography in the evaluation of head injury. Neurosurgery 1986;18(1):45–52. [PubMed]

Additional information and reprint requests:
Emin Aghayev, M.D.
University of Bern
Institute of Forensic Medicine
IRM–Buehlstrasse 20
CH–3012 Bern
Switzerland
E-mail: emin.aghayev@irm.unibe.ch